ISTP

RESEARCH ARTICLE

Experimental Study on Entropy Features in Machining Vibrations of A Thin-Walled Tubular Workpiece

Kaibo Lu,[1] Xin Wang,[1] Xun Chen,[2] Xinyu Pang,[1] and Fengshou Gu[3]

[1]College of Mechanical and Vehicle Engineering, Taiyuan University of Technology, Shanxi 030024, China
[2]General Engineering Research Institute, Liverpool John Moores University, Liverpool, L3 5UX, UK
[3]School of Computing and Engineering, University of Huddersfield, Huddersfield, HD1 3DH, UK

Abstract: In machining processes, chatter vibrations are always regarded as one of the major limitations for production quality and efficiency. Accurate and timely monitoring of chatter is helpful to maintain stable machining operations. At present, most chatter monitoring methods are based on the energy level at specified chatter frequencies or frequency bands. However, the spectral features of chatter could change during machining operations due to complexity and time-varying dynamics of the physical machining process. The purpose of this paper is to investigate the time-varying chatter features in turning of thin-walled tubular workpieces from the perspective of entropy. The airborne acoustics was selected as the source of information for machining condition monitoring. First, corresponding to the distinguishing surface topographies relevant to machining conditions, the features of the sound signal emitted during turning of the thin-walled cylindrical workpieces were extracted using the spectral analysis and wavelet packet transform, respectively. It was shown that the dominant vibration frequency as well as the energy distribution could shift with the transition of the machining status. After that, two relative entropy indicators based on the spectrum and the wavelet packet energy were constructed to identify chattering events in turning of the thin-walled tubes. The experimental results demonstrate that the proposed indicators could accurately reflect the transition of machining conditions with high sensitivity and robustness in comparison with the traditional FFT-based methods. The achievement of this study lays the foundations of the online chatter monitoring and control technique for turning of the thin-walled tubular workpieces.

Keywords: machining; chatter; relative entropy; thin-walled workpieces

I. INTRODUCTION

During cutting of flexible parts like thin-walled flanges or long slender shafts, machining chatter vibrations are prone to occurrence due to the insufficient stiffness of machine tool-workpiece systems or the unreasonable setting of cutting parameters [1,2]. Chatter is a self-excited vibration between the tool and the workpiece in machining processes, leading to poor surface quality and low production efficiency. Therefore, it is of great significance to monitor the machining condition for identifying the occurrence of chatter accurately and quickly, thereby ensuring the stability of the process.

The procedure for chatter detection mainly includes three aspects: signal acquisition, feature extraction, and state recognition [3]. The widely used sources of information on chatter are the process variables affected by the material removal progression. The most frequently measured signals are force [4], vibration [5–7], acoustics [8,9], current, or power [10,11]. Compared to other signals, cutting forces were regarded as more suitable for chatter detection, because this physical variable can directly characterize the dynamic interaction between the tool and the workpiece. Cardi *et al.* [4] proposed the phase difference between the cutting force and the workpiece velocity to identify the onset of chatter in turning operations. Lu *et al.* [5] developed a comprehensive indicator for chatter monitoring when turning a long slender shaft, which integrates

the time domain variance and spectral features of acceleration signals. Li *et al.* [7] developed a novel three-axis wireless on-rotor acceleration sensing system for monitoring the turning process. Delio *et al.* [8] adopted airborne acoustics to detect milling chatter and proved that a microphone could provide proper and consistent signals for reliable chatter detection and control in comparison with dynamometers, displacement sensors, and accelerometers. In addition, Lamraoui *et al.* [10] used current signals to monitor chatter during milling operations, in which the original signal was processed by data mining techniques to amplify and extract chatter features.

In terms of signal processing for chatter detection, the methods were largely divided into two scopes including the time domain analysis and the time-frequency domain analysis [1–3]. Ye *et al.* [12] proposed vibration waveform irregular coefficients according to the ratio of the standard deviation to the mean to predict the early machining chatter. Time-frequency analysis methods were also widely used in the feature extraction of chatter vibrations, which consist of the short-time Fourier transform [13], wavelet transform [14,15], and empirical mode decomposition [16]. Liu *et al.* [15] introduced the normalized spectral entropy and logarithmic spectral distance using cross-wavelet transform for grinding chatter identification. The results showed that the proposed indicators could perform self-adaptive monitoring for chatter. With the development of artificial intelligence, several classification models based on machining learning have also been applied for chatter recognition, such as the neural network models [17], support vector machine models [18], and hidden Markov models [19].

Corresponding author: Kaibo Lu (e-mail: lvkaibo@tyut.edu.cn).

In summary, a number of productive outcomes have been achieved in the area of machining chatter monitoring. However, the issue of turning of the challenging thin-walled tubular workpieces has rarely been involved. Compared with solid structures, the dynamic characteristics of thin-walled workpieces seem to be more sensitive to the removal of material during cutting [20–22]. In addition, the thin-walled tubular workpiece subjected to external forces generally vibrates in combination of the beam and shell modes [23]. These differences make the response of the vibratory thin-walled tubular structure time-varying and complex, leading to a difficulty in judging the machining condition accurately.

In this paper, we introduce the relative entropy to deal with the complexity of machining vibrations when turning a thin-walled tubular workpiece so as to characterize the changing condition of the process. Two relative entropy indicators for condition monitoring are proposed using the wavelet packet energy and the spectrum of vibration signals generated in cutting operations. Finally, machining trials of thin-walled tubes were conducted to verify the effectiveness of the developed entropy indicators for chatter detection.

II. RELATIVE ENTROPY

The relative entropy is an asymmetric measure of the difference between two probability distributions, which can be used to measure similarity between two random distributions. The greater the relative entropy value, the larger the difference between the two random distributions; on the contrary, the smaller the value, the closer the two random distributions; if and only if two random distributions are exactly the same, the relative entropy value equals zero.

if $P(x)$ and $Q(x)$ are two probability distributions on a random variable x, where $P(x)$ is the true distribution, and $Q(x)$ is the ideal distribution or fitted distribution, then in the case of discrete and continuous random variables, the relative entropy of $P(x)$ with respect to $Q(x)$ is defined respectively as:

$$KL(P\|Q) = \sum P(x) \log \frac{P(x)}{Q(x)} \quad (1)$$

$$KL(P\|Q) = \int P(x) \log \frac{P(x)}{Q(x)} dx \quad (2)$$

A. RELATIVE WAVELET PACKET ENERGY ENTROPY

As an extension of the wavelet transform, the wavelet packet transform (WPT) can decompose the signal in both the low-frequency band and the high-frequency band with better time-frequency local analysis. A schematic diagram of the wavelet packet decomposition is shown in Fig. 1.

In the WPT method for m-level decomposition, the original signal can be divided into 2^m frequency bands. Because the sequence of each frequency band after wavelet packet decomposition is not strictly arranged according to node numbers, after reordering the frequency range at level m and band i is

$$[(i-1)2^{-m}f, i \cdot 2^{-m}f] \quad i = 1,2,\ldots 2^m \quad (3)$$

where f is the Nyquist frequency of the signal.

The wavelet packet coefficient corresponding to the frequency band is defined as

$$x_m^i = \left\{ c_{i,j}, j = 1,2,\ldots K \right\} \quad i = 1,2,\ldots 2^m \quad (4)$$

where K is the total number of discrete points of the signal wavelet packet transformation in this frequency band. Thus, the energy of node i at level m has

$$E_{m,i} = \sum_{j=1}^{K} |c_{i,j}|^2 \quad (5)$$

The total energy E of all frequency bands can be expressed as

$$E = \sum_{i=1}^{2^m} E_{m,i} \quad (6)$$

The ratio of each frequency band energy $E_{m,i}$ to the total energy E is defined as the proportion of energy, which is expressed as

$$p_i = \frac{E_{m,i}}{E} \quad (7)$$

The measured signal $x_l(t)$ is decomposed into m levels, and the proportion of energy in each frequency band can be calculated. The signal energy probability distribution is $P_l = \{p_1^l, p_2^l, \cdots, p_{2^m}^l\}$. Meanwhile, the energy probability distribution of the signal generated during stable cutting is taken as the reference distribution $P_r = \{p_1^r, p_2^r, \cdots p_{2^m}^r\}$.
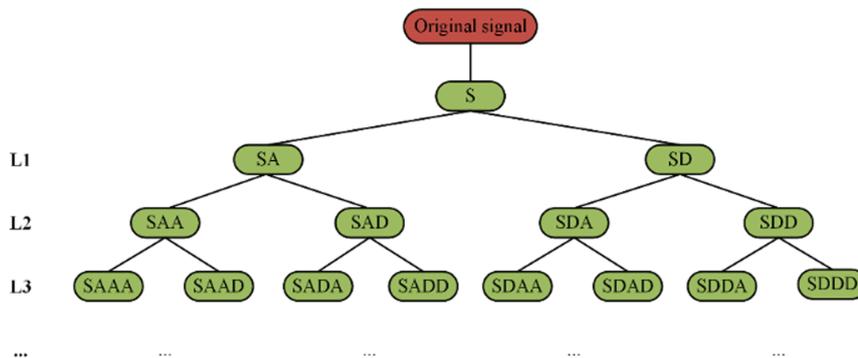
Fig. 1. Schematic diagram of wavelet packet decomposition.

According to Eq. (1), the relative entropy of wavelet packet energy is defined as

$$KL(P_l \| P_r) = \sum_{i=1}^{2^m} p_i^l \log \frac{p_i^l}{p_i^r} \qquad (8)$$

where p_i^l is the energy ratio of the i*th* band at the l*th* time segment, and p_i^r is the energy proportion of the i*th* band for the reference distribution.

B. RELATIVE SPECTRAL ENTROPY

The measured signal $x_l(t)$ with the length of $2L$ is transformed using the Fast Fourier Transform (FFT) to obtain its spectrum. The number of spectral lines is L. After normalizing the amplitude corresponding to each line to calculate the proportion of amplitude, we can obtain the spectral probability distribution $A_l = \{a_1^l, a_2^l, \cdots, a_L^l\}$. Furthermore, the spectral probability distribution of the stable cutting signal is also regarded as the reference distribution $A_r = \{a_1^r, a_2^r, \cdots a_L^r\}$.

According to Eq. (1), the relative entropy of FFT spectrum is defined as

$$KL(A_l \| A_r) = \sum_{i=1}^{L} a_i^l \log \frac{a_i^l}{a_i^r} \qquad (9)$$

where a_i^l is the proportion of the amplitude of the i*th* spectral line at the l*th* time segment, and a_i^r is the proportion of amplitude with respect to the i*th* spectral line for the reference distribution.

III. EXPERIMENTAL SETUP AND MODAL MEASUREMENT

A. EXPERIMENTAL SETUP

In order to verify the effectiveness of the relative entropy for chatter identification in machining of thin-walled tubular workpieces, experimental tests were carried out on a CA6140 lathe, as shown in Fig. 2. Two typical thin-walled tubes with different geometric dimensions were chosen and presented for comparison. During machining, the thin-walled cylinder was fixed at one end and free at the other end, and the feed direction of the tool was from the chuck side to the free end. The clamping length by the three-jaw chuck was 40 mm. The type of the tool holder was SDNCN25 * 25M11, and the corresponding tool insert was DCMT11T304. The workpiece material was AISI 1,040. An accelerometer was
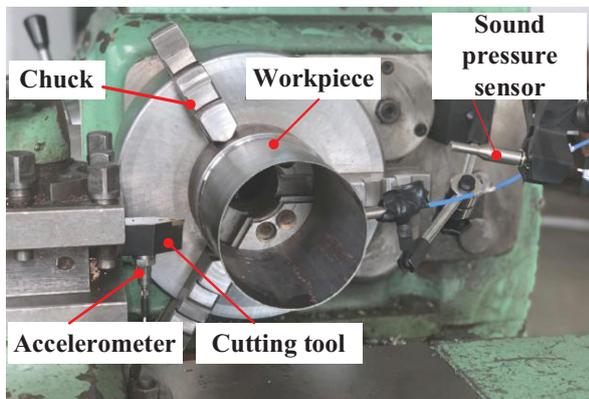
Fig. 2. Experimental layout for machining tests.

Table I.   Main cutting parameters in the experiments

Tube	A	B
Length (mm)	195	160
Wall thickness (mm)	1.5	1.3
Inner diameter (mm)	111	130
Spindle rotation speed (rpm)	740	583
Depth of cut (mm)	0.8	0.6
Feed rate (mm/rev)	0.1	0.1
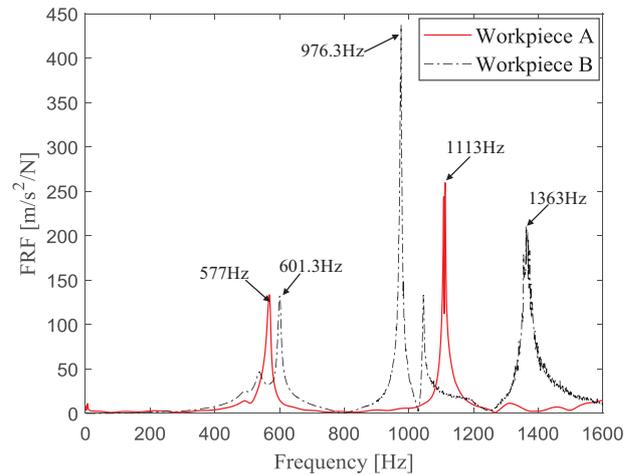
Fig. 3. Measured FRFs of the two workpieces.

attached to the back of the tool and a sound pressure sensor supported by a bracket was placed next to the lathe. The sample rate of the data acquisition (DAQ) was 10.24 kHz. The main cutting parameters for the experiments are summarized in Table I.

B. MODAL MEASUREMENTS

The modal measurements were conducted before the cutting tests. Compared with the rigidity of the tool, the cantilevered tube was regarded as the only compliant component in the machining system. Figure 3 presents the frequency response functions (FRFs) of the two workpieces. It can be seen that for Tube A, there are two peaks at 577 Hz and 1113 Hz in the spectrum, which correspond to the first two Eigen frequencies of the thin-walled workpiece; for Tube B, the first three natural frequencies are 601.3 Hz, 976.3 Hz, and 1,363 Hz, respectively.

IV. RESULTS AND DISCUSSION

A. PRELIMINARY ANALYSIS OF THE SIGNALS

Figure 4 shows the comparison of the airborne acoustics and acceleration generated during cutting. It can be seen that when chatter occurred, the amplitude of the acoustic signal varied more significantly than that of the acceleration signal. Moreover, as shown in Fig. 5, the time-frequency spectrum of the acceleration was obviously complex in the high-frequency band (red dotted box), indicating that the accelerometer was more sensitive to the high-frequency vibration.

(a)

(b)
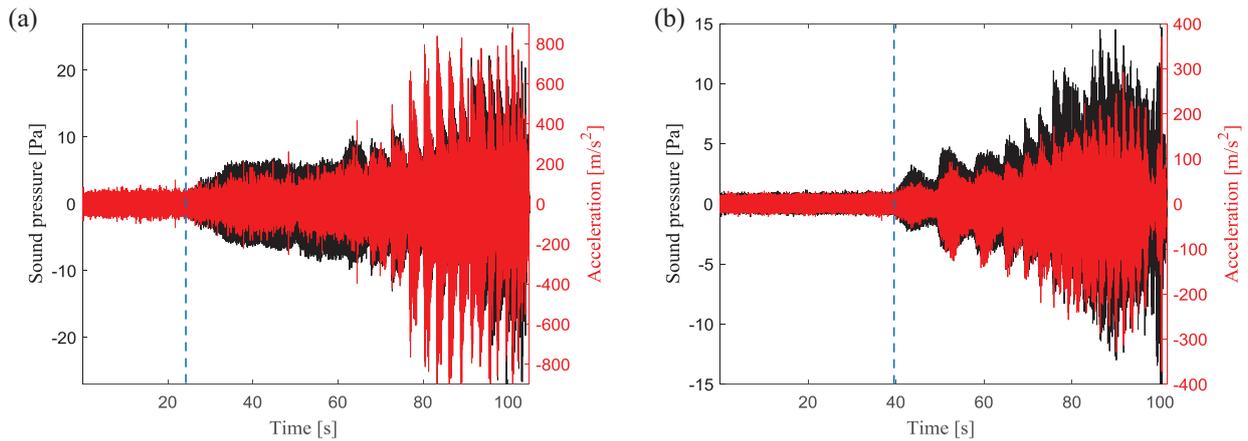
Fig. 4. Comparison of the sound and acceleration signals in the time domain. (a) Tube A. (b) Tube B.

(a)

(b)
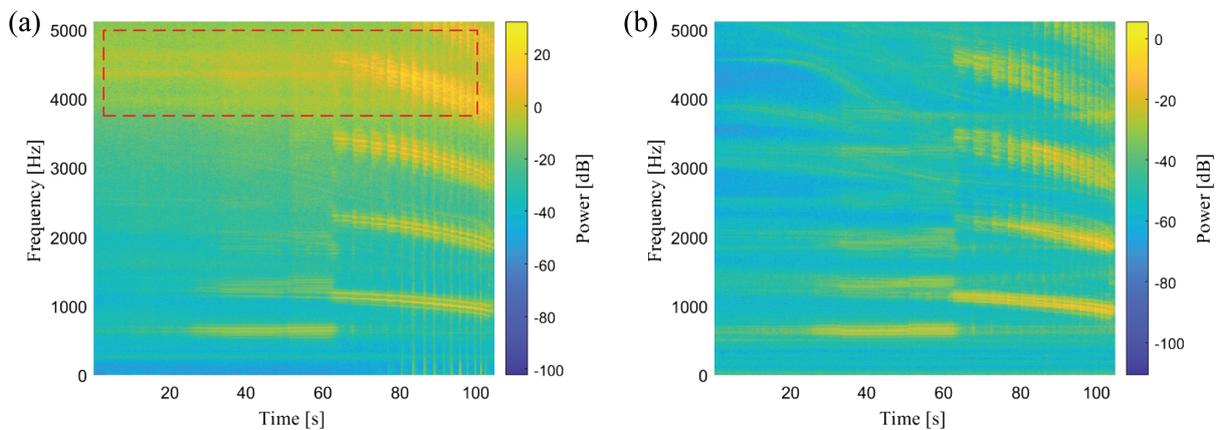
Fig. 5. Comparison of the time-frequency analysis of the acceleration (a) and the sound (b) for Tube A.

This complexity in spectrum could distract the identification of chatter frequency. When compared with accelerometers, the sound sensors also have the advantages of easy installation and remote non-contact measurement. Thus, the acoustic signal was selected for processing and analysis in the subsequent sections.

Observing the acoustic waveform and its spectrum, we can see that at the beginning of cutting the amplitude of sound was small and the cutting process was stable; after a moment, the amplitude began to increase and fluctuate, indicating the process became unstable. This transition is because the compliance of the thin-walled workpiece near its free end is higher than that near its clamped side. When chatter happened, the high-frequency components dominated in the spectrum. The dominant vibration frequency could be decreased gradually as the cutting progressed, as shown in Fig. 5b.

B. CHATTER FEATURE EXTRACTION

According to the machined patterns as well as the surface roughness measurements of Tube A, three different zones were divided, including the stable cutting, slight chatter, and severe chatter zones, as shown in Fig. 6a. Correspondingly, the sound waveform as well as its spectrum along the cutting path exhibited different features, as seen in Fig. 6.

In order to determine the distribution of the spectrum and the wavelet packet energy in different machining conditions, the segmented data from each condition were
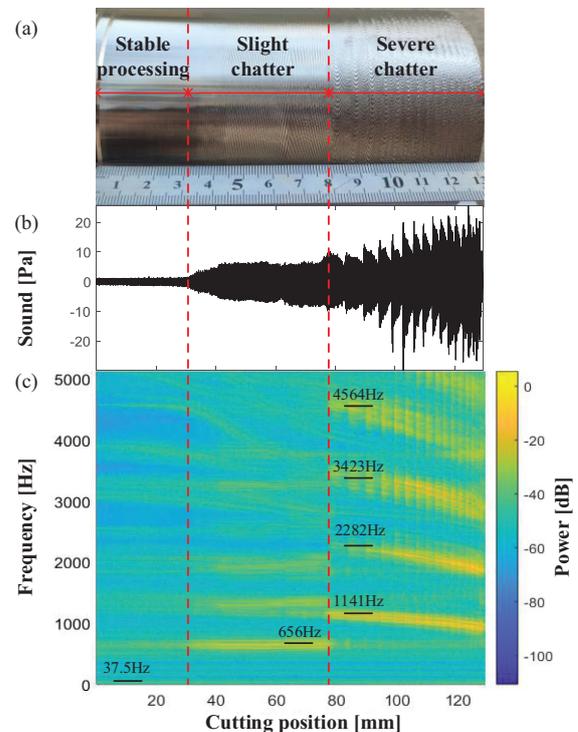
Fig. 6. Machined surface quality and signal features along the cutting path of Tube A. (a) Surface textures. (b) Sound signals. (c) Spectra of the sound.

processed for comparison. The corresponding cutting positions along the axis of the workpiece were at S1 (3.7–4.9 mm), S2 (49.3–50.6 mm), and S3 (98.7–99.9 mm), respectively. For the wavelet packet energy calculation, the level of WPT was set to be 5, and the interval of the frequency band was 160 Hz. The signal processing results are presented and compared in Figs. 7–9.

At the stable cutting area S1, the analysis results through FFT and WPT are shown in Fig. 7. It is seen that the dominant frequency with the largest amplitude in the spectrum was 36.88 Hz, which was about three times of

the spindle rotational frequency. Meanwhile, the energy distribution was concentrated at the wavelet packet node 1 with the frequency range of 0–160 Hz.

At the slight chatter area S2, the signal processing results using FFT and WPT are shown in Fig. 8. As seen in Fig. 8(b), the dominant frequency with the largest amplitude in the spectrum was around 664.5 Hz, which is a little higher than the first natural frequency of the workpiece shown in Fig. 3. Besides, there were other frequency components such as the harmonics of the dominant chatter frequency and the rotational frequency. Figure 8c shows
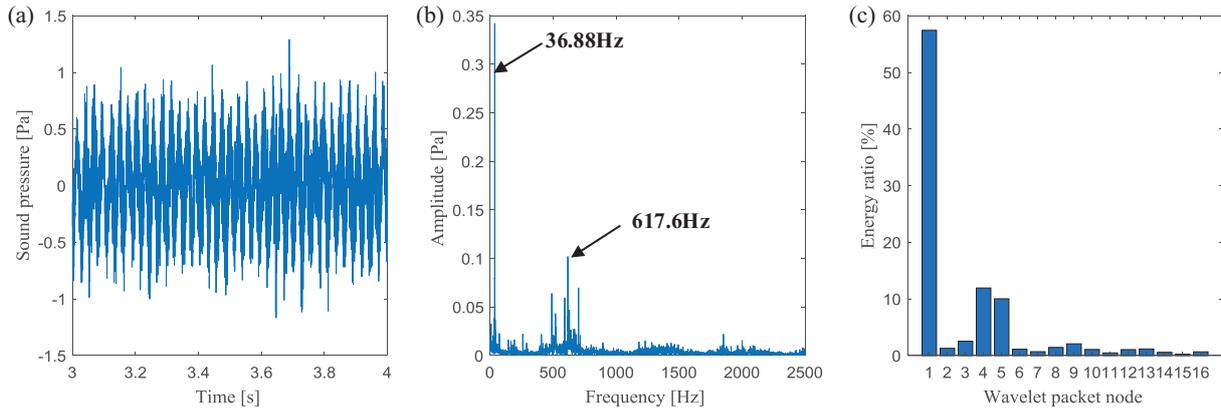
Fig. 7. Sound waveform (a), spectral analysis (b), and wavelet packet energy distribution (c) at S1.
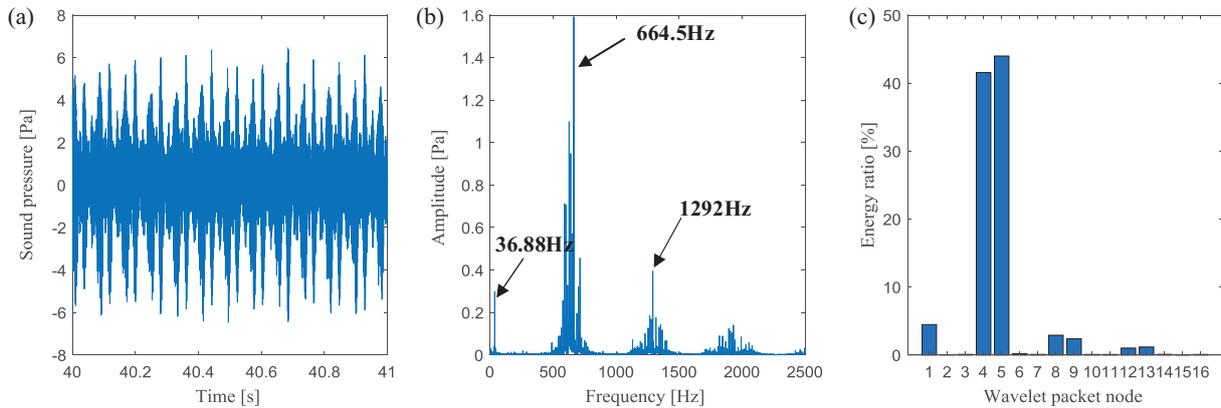
Fig. 8. Sound waveform (a), spectral analysis (b), and wavelet packet energy distribution (c) at S2.
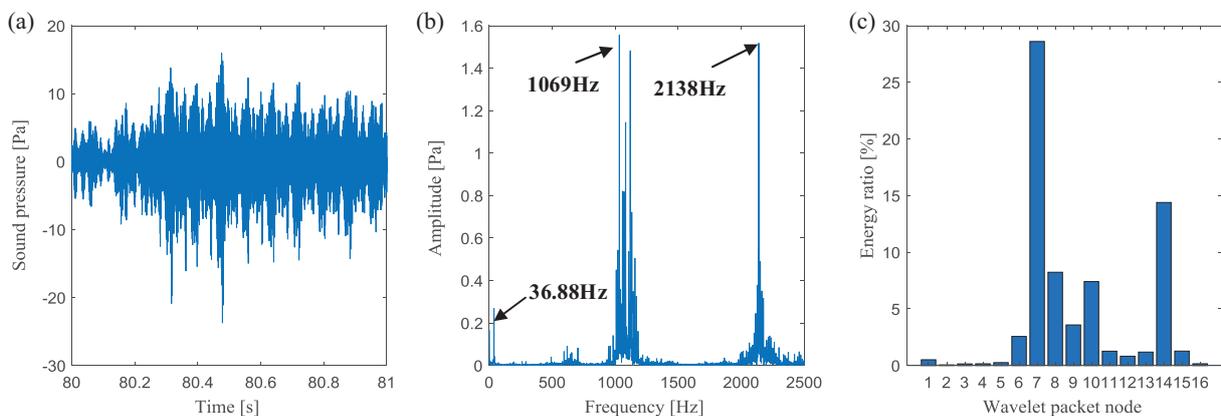
Fig. 9. Sound waveform (a), spectral analysis (b), and wavelet packet energy distribution (c) at S3.

that the corresponding energy distribution was concentrated at the wavelet packet nodes 4 and 5 with the frequency range of 480–800 Hz.

At the severe chatter area S3, the analysis results are shown in Fig. 9. It is interesting to note that the dominant chatter frequency jumped from 664.5 Hz to around 1,069 Hz accompanied by its harmonics, which is close to the second natural frequency of the workpiece shown in Fig. 3. Apparently, the chatter detection methods based on scanning for chatter frequencies in a specified band, such as references [14–16], could be unreliable due to the spectral shift. Besides, the harmonics of the dominant chatter frequency and the rotational frequency also occurred. Figure 9c shows that the energy distribution was concentrated at nodes of 7–8 corresponding to the frequency range of 960–1280 Hz and at node 14 with the frequency range of 2080–2140 Hz.

It is concluded that the dominant vibration frequency as well as the energy distribution shifted with the transition of the machining status during machining of Tube A, leaving distinct chatter marks on the machined surface. The physical mechanism behind these phenomena could be that the moving contact point between the cutting tool and the workpiece in operation leads to time-varying and position-dependent dynamics of the machining system, which critically determines the chatter stability of machining processes [24–26].

For turning of Tube B, the surface quality and the signal processing results are shown in Fig. 10, in which the chatter patterns are similar to the results in [27,28]. In comparison with Tube A case, it is seen that only one kind of chatter patterns left on the machined surface and the chatter frequency shift phenomenon did not happen in this case. The reason probably is that under this chattering condition, the machined tube could always vibrate in its solo weakest mode which held the minimum of the real part of the receptance frequency response function.
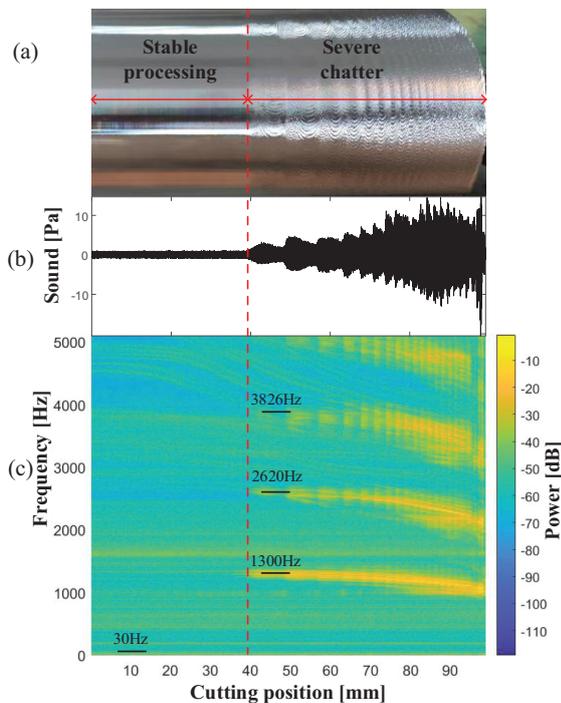
C. RELATIVE ENTROPY RESULTS

In this section, the proposed two entropy indicators, including the relative entropy of the wavelet packet energy and the spectrum, were tested for detection of the time-varying chattering status as depicted above. One block of data acquired in the initial period of stable cutting was taken as the benchmark. The difference between the target probability distribution and the reference distribution was then calculated to characterize the fluctuations of cutting conditions in the subsequent time. For signal processing, the overlap processing technique was used to speed up the calculation. The number of samples in the sliding frame for processing was 1,280, and the overlap ratio was set to 50%.

The relative entropy with respect to the cutting position along the length of the workpiece was compared with the traditional time-frequency analysis result, as shown in Figs. 11, 12, where the colorbars facing the right axes display the amplitude of the chattering frequency component. It is readily seen that during the stable cutting the relative entropy was low, whereas the value was increased significantly when chatter happened. Especially, at the location where the dominant vibration frequency shifted, the corresponding relative entropy showed jumps sensitively at the onset of chatter. In addition, the proposed relative entropy indicators could trigger an earlier alarm for
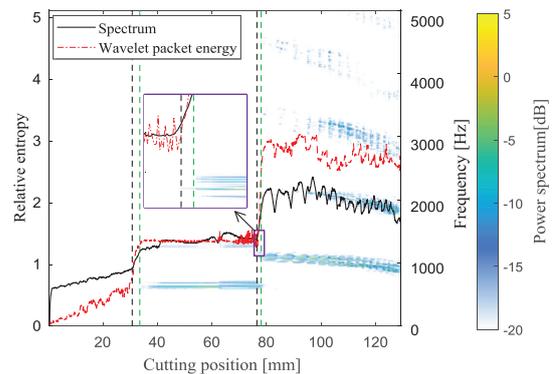
Fig. 11. Comparison of the relative entropy method and the FFT-based method for chatter detection of Tube A.

Fig. 10. Machined surface quality and signal features along the cutting path of Tube B. (a) Surface textures. (b) Sound signals. (c) Spectra of the sound.
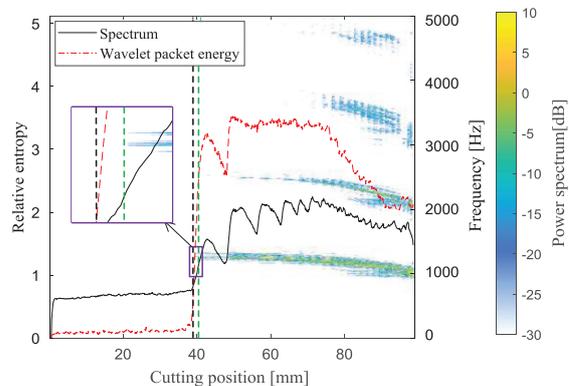
Fig. 12. Comparison of the relative entropy method and the FFT-based method for chatter detection of Tube B.

chatter monitoring when compared with the traditional power spectrum (see the enlarged portions in Figs. 11, 12).

As shown in Fig. 11 regarding Tube A, at the stage of the slight chatter development, the relative entropy indicators using both the wavelet packet energy and the spectrum of the sound signal nearly remained constant. At the stage of the severe chatter, however, the two indicators showed evident fluctuations. The similar scenario can be found in Fig. 12 regarding Tube B. This indicates that the dynamic behaviors of the machining system underwent strong time variation in the period of the severe chatter vibration.

Overall, the proposed relative entropy indicators could allow the event of machining condition transition to be identified accurately in turning of the thin-walled tubular workpieces. Comparatively, the relative entropy of the wavelet packet energy showed higher sensitivity and robustness to the chatter shift events.

V. CONCLUSION

This paper presents an experimental investigation on the vibration features from the perspective of entropy when turning a thin-walled tubular workpiece. Airborne sound was chosen as the source of information by means of the advantages of global sensing measurement and easy installation of the sound sensors. Considering that the relative entropy can measure the similarity between the target distribution and the reference distribution, two relative entropy indicators based on the WPT and Fourier transform were developed for machining condition monitoring. The experimental results show that the dominant vibration frequency as well as the energy distribution could shift with the transition of the machining status during turning of the thin-wall tubes, resulting in distinguishing topographies on the machined surface. It is demonstrated that the proposed relative entropy of spectrum and wavelet packet energy could detect the event of transition of machining conditions with higher sensitivity and accuracy in comparison with the traditional FFT-based method for chatter monitoring. This investigation lays the foundations of the online chatter control technique for turning of the thin-walled cylindrical components.

Acknowledgments

CONFLICT OF INTEREST STATEMENT

The authors declare no conflicts of interest.

References

[1] J. Munoa, X. Beudaer, Z. Dombovari, Y. Altintas, E. Budak, C. Brecher, and G. Stepan, "Chatter suppression techniques in metal cutting," CIRP Ann.-Manuf. Technol., vol. 65, pp. 785–808, 2016.

[2] G. Wu, G. Li, W. Pan, I. Raja, W. Wang, and S. Ding, "A state-of-art review on chatter and geometric errors in thin-wall machining processes," J. Manuf. Process., vol. 68, pp. 454–480, 2021.

[3] G. Urbikain, D. Olvera, L.N. Lopez de Lacalle, A. Beranoagirre, and A. Elias-Zuniga, "Prediction methods and experimental techniques for chatter avoidance in turning systems: a review," Appl. Sci.-Basel, vol. 9, p. 4718, 2019.

[4] A. A. Cardi, H. A. Firpi, M. T. Bement, and S. Y. Liang, "Workpiece dynamic analysis and prediction during chatter of turning process," Mech. Syst. Signal Process., vol. 22, pp. 1481–1494, 2008.

[5] K. Lu, Z. Lian, F. Gu, and J. Liu, "Model-based chatter stability prediction and detection for the turning of a flexible workpiece," Mech. Syst. Signal Process., vol. 100, pp. 814–826, 2018.

[6] G. Stepan, A. K. Kiss, B. Ghalamchi, J. Sopanen, and D. Bachrathy, "Chatter avoidance in cutting highly flexible workpieces," CIRP Ann. –Manuf. Technol., vol. 66, pp. 377–380, 2017.

[7] C. Li, Z. Zou, K. Lu, H. Wang, R. Cattley, and A.D. Ball, "Assessment of a three-axis on rotor sensing performance for machining process monitoring: a case study," Sci. Rep. vol. 12, p. 16813, 2022.

[8] T. Delio, J. Tlusty, and S. Smith, "Use of audio signals for chatter detection and control," J. Manuf. Sci. Eng., vol. 114, pp. 146–157, 1992.

[9] J. Gao, Q. Song, and Z. Liu, "Chatter detection and stability region acquisition in thin-walled workpiece milling based on CMWT," Int. J. Adv. Manuf. Technol., vol. 98, pp. 699–713, 2018.

[10] M. Lamraoui, M. Badaoui, and F. Guillet, "Chatter detection in CNC milling processes based on Wiener-SVM approach and using only motor current signals," in Vibration Engineering and Technology of Machinery, editor: Jyoti K. Sinha, Cham: Springer, 2015, pp. 567–578.

[11] D. Aslan and Y. Altintas, "On-line chatter detection in milling using drive motor current commands extracted from CNC," Int. J. Mach. Tools Manuf., vol. 132, pp. 64–80, 2018.

[12] J. Ye, P. Feng, C. Xu, Y. Ma, and S. Huang, "A novel approach for chatter online monitoring using coefficient of variation in machining process," Int. J. Adv. Manuf. Technol., vol. 96, pp. 287–297, 2018.

[13] R. Thomazella et al., "Digital signal processing for self-vibration monitoring in grinding: a new approach based on the time-frequency analysis of vibration signals," Measurement, vol. 145, 2019, pp. 71–83.

[14] K. Lu, P. Lou, F. Gu, W. Pan, and Z. Chang, "Study on early chatter monitoring based on energy kurtosis index of acoustic signals," J. Vib. Shock, vol. 40, no. 20, pp. 50–55, 2021.

[15] Y. Liu et al., "An adaptive grinding chatter detection method considering the chatter frequency shift characteristic," Mech. Syst. Signal Process., vol. 142, p. 106672, 2020.

[16] H. Cao, Y. Lei, and Z. He, "Chatter identification in end milling process using wavelet packets and Hilbert–Huang transform," Int. J. Mach. Tools Manuf., vol. 69, pp. 11–19, 2013.

[17] S. Kumar and B. Singh, "Chatter prediction using merged wavelet denoising and ANFIS," Soft Comput., vol. 23, no. 12, pp. 4439–4458, 2019.

[18] Y. Wang et al., "Mirror milling chatter identification using Q-factor and SVM," Int. J. Adv. Manuf. Technol., vol. 98, no. 5, pp. 1163–1177, 2018.

[19] Z. Han, H. Jin, and H. Fu, "Modeling of chatter recognition system in CNC milling based on ESPRIT and hidden Markov model," Comput. Integr. Manuf. Syst., vol. 22, no. 8, pp. 1938–1944, 2016.

[20] G. J. Lai and J. Y. Chang, "Stability analysis of chatter vibration for a thin-wall cylindrical workpiece," Int. J. Mach. Tools Manuf., vol. 35, no. 3, pp. 434–444, 1995.

[21] K. Mehdi, J. F. Rigal, and D. Play, "Dynamic behavior of a thin-walled cylindrical workpiece during the turning – cutting process, Part 1: Cutting process simulation," J. Manuf. Sci. Eng., vol. 124, no. 3, pp. 562–568, 2002.

[22] C. X. Wang, X. W. Zhang, X. F. Chen, and H. R. Cao, "Time-varying chatter frequency characteristics in thin-Walled workpiece milling with B-Spline wavelet on interval finite element method," J. Manuf. Sci. Eng., vol. 141, no. 5, p. 051008, 2019.

[23] X. M. Zhang, G. R. Liu, and K. Y Lam, "Vibration analysis of thin cylindrical shells using wave propagation approach," J. Sound Vib., vol. 239, pp. 397–403, 2001.

[24] K. Cheng, "Machining dynamics: fundamentals," in Applications and Practices, editor: Kai Cheng, London: Springer, 2009.

[25] Y. Altintas, Manufacturing Automation: Metal Cutting Mechanics, Machine Tool Vibrations and CNC Design. Cambridge: University Press, 2012.

[26] K. Lu, F. Gu, A. Longstaff, and G. Li, "An investigation into tool dynamics adaptation for chatter stability enhancement in the turning of flexible workpieces," Int. J. Adv. Manuf. Technol., vol. 111, pp. 3259–3271, 2020.

[27] K. Mehdi, J. Rigal, and D. Play, "Dynamic behavior of a thin-walled cylindrical workpiece during the turning process, Part 2: experimental approach and validation," J. Manuf. Sci. Eng., vol. 124, no. 3, pp. 569–580, 2002.

[28] A. Gerasimenko, M. Guskov, A. Guskov, P. Lorong, and A. Shokhin, "Analytical modeling of a thin-walled cylindrical workpiece during the turning process. Stability analysis of a cutting process," J. Vibroeng., vol. 19, no. 8, pp. 5825–5841, 2017.